

## IMPROVEMENT OF THE ENERGY UTILIZATION EFFICIENCY OF THE V-Ti-MAGNETITE REDUCTION PROCESS WITH ROTARY HEARTH FURNACE

R. Wei, Z. Lun, X. Lv\*, T. Hu, C. Bai

College of Materials Science and Engineering, Chongqing University, China

(Received 28 December 2012; accepted 27 October 2014)

### Abstract

*In order to improve the energy utilization of rotary hearth furnace (RHF), some methods were raised to solve the problem. Through changing the inlet angle of the nozzle, a higher and more uniform temperature field can be got. Thus, the burden in the furnace can be heated to the reduction temperature in a relatively shorter time. By using multilayer pellets technology, the energy can be utilized as much as possible. However, the top layer pellets would be reoxidized when the middle and bottom layer pellets were reduced. The average metallization of the reduced pellets get the maximum value at 25 min, which is consistent with the reality operation.*

*Keywords: energy utilization; RHF; reoxidation; inlet angle; V-Ti-Magnetite*

### 1. Introduction

There is about 10 billion tonnage of iron ore deposit called vanadium titanomagnetite, in Panzhihua area, southwest of China. The average content of Fe and TiO<sub>2</sub> is about 30% and 9%, respectively in the original mineral. The magnetite concentrate and the ilmenite concentrate are the two main products after the beneficiation process, whose classical chemical compositions are shown in Table 1. For the BF-BOF process, the elements such as Fe and V in magnetite concentrate are both reduced into hot metal, while most of the titanium in the concentrate was not reduced and remained in the slag.

**Table 1.** Chemical composition of the magnetite and ilmenite (wt.%)

Components	TFe	FeO	TiO <sub>2</sub>	V <sub>2</sub> O <sub>5</sub>	SiO <sub>2</sub>	Al <sub>2</sub> O <sub>3</sub>	MgO	CaO
Magnetite	53~55	20~23	12~13	0.561	5.01	4.8	3.67	1.53
Ilmenite	32~34	34~36	45~49	0.068	1.29	1.34	4.8	0.72

Titanium is a very important and useful metal which is widely used in the aerospace and chemical industrial. Many countries consider deposits of titanium as a strategic resource. China is abundant in titanium, account for about 48% of the world. However, the recovery rate of the titanium is much low in the current process of the vanadium titanomagnetite resources. About 54% titanium

contained in the magnetite concentrate converts into blast furnace slag with little usage, because the utilization of the blast furnace slag containing high TiO<sub>2</sub> is a big difficulty. In the view of recovery of titanium, 20~25% TiO<sub>2</sub> is neither high for directly utilization nor low to drop off. A new process is necessary to develop and the recovery rates of all the metal elements require improvement. Therefore, the RHF followed by the EAF process was suggested to deal with the V-Ti-Magnetite as an available method [1-2]. The TiO<sub>2</sub> content in the EAF slag after smelting process can reach to as high as 48% due to the useless of the flux, which can be used as the raw materials for recovery TiO<sub>2</sub>. The RHF-EAF process has been installed in Panzhihua area, China with an annual DRI production of 100000 tonnages [3-5]. However, the energy utilization efficiency of the RHF is low which will be a great disadvantage for the further application. There is only one layer of pellets on the hearth of the RHF currently. The multi-layer pellets pattern would improve the energy utilization efficiency of the RHF [5], in which pattern the synchronization reduction among the individual layers is the key point [6]. The heat transfer pattern in current RHF process mostly depends on the radiation heat, the lower layer of pellets are hardly to be radiated. Therefore, the heat transfer pattern should be modified to fit the multi-layer burden.

In present study, the heat transfer pattern was studied from the view of changing the injection angle of the natural gas and air for increasing the convection heat transfer to the lower layer of pellets.

\* Corresponding author: lxuwei@163.com

## 2. The influence of injection angle on the heat transfer pattern

In the current state of RHF, the burners in the wall are all designed to the horizontal direction; the pellets are heated by the radiation of the high temperature flame. For the multi-layers of pellet, the lower layer of pellets is hardly to be radiated, resulting low heating rate and low reduction degree of the iron. For improving the heating rate of the lower pellets, the injection direction of the burner can be modified to the low part of the furnace.

The influence of the injection angle on the heat transfer pattern was simulated with the fluid dynamic software-Fluent. The sketch map of different injection angles were shown in Fig.1. The cases simulated were shown in Table 2.

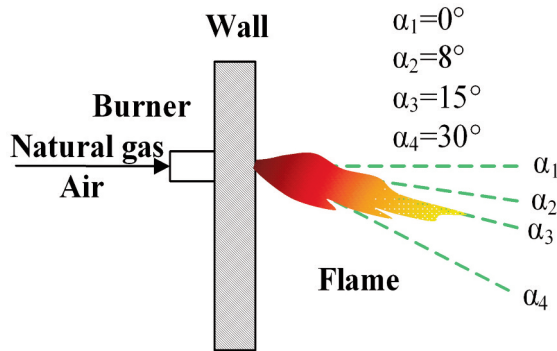


Figure 1. Sketch map of different injection angles

The atmosphere in the experiment was fixed as:  $CO_2/CO=2$ , the required amount of natural gas and air were then determined. After the temperature field was stable, the off-gas was analyzed online by gas analyzer. The experimental apparatus was shown in Fig. 2.

The simulated results were shown in Fig.3, 4 and 5. Fig. 3 shows the sectional view of the center of Y axis. It exhibits that when  $\alpha$  equals to  $8^\circ$  and  $15^\circ$ , the high temperature area move down obviously, the burden will be heated in a very short time in such case; while  $\alpha$  equals to  $30^\circ$ , the area of the high temperature presents a shrink tendency

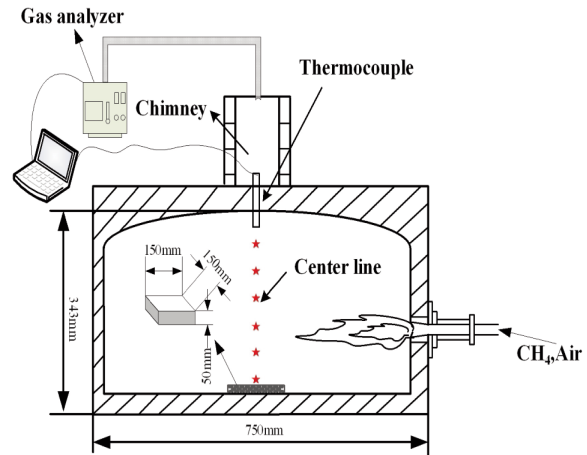


Figure 2. Experimental apparatus

and the temperature field have a non-uniform distribution on the burden surface which is definitely bad to the quick heating of the burden.

Fig. 4 shows the sectional view of the surface of  $Z=25mm$  with different  $\alpha$ . It indicates that the zone of high temperature expands where  $Z=25mm$  with  $\alpha$  from 0 to  $15^\circ$ , However the high temperature zone moves to the back of the furnace, resulting the un-uniform heating rate between the right and left part of the injection direction of the natural gas.

The temperature distribution along the center line (as shown in Fig. 2) with different  $\alpha$  in steady state was also discussed which was shown in Fig. 5. The high temperature area would move towards to the bottom surface and become nearer to the nozzle in horizontal direction with increasing the  $\alpha$ . When  $\alpha$  equals to  $8^\circ$ , the highest temperature appears at the point of  $Z=8cm$  and that is 5cm when  $\alpha$  equals to  $15^\circ$ . In consideration of the common thickness of burden in RHF was less than 50mm, the temperature of the burden can be raised up at the shortest time while  $\alpha$  equals to  $15^\circ$ . When  $\alpha$  equals to  $30^\circ$ , the high temperature area has already far away from the center burden and some burden will go away with the flue gas due to the violent washing from the high speed inlet airstream.

Table 2. Simulated case and the boundary conditions

Injection angle( $\alpha$ )	Reaction equation	Boundary conditions
$0^\circ, 8^\circ, 15^\circ, 30^\circ$	$3.674CH_4 + 6.405O_2 = 1.027CO + 2.647CO_2 + 0.859H_2 + 6.489H_2O$	Wall temperature = $1300^\circ C$
		Inlet velocity = 2.86m/s
		Inlet mass fraction: $CH_4\% = 0.06$ ; $O_2\% = 0.22$
		Outlet mass fraction: $CO\% = 0.031$ ; $CO_2\% = 0.124$ ; $H_2\% = 0.002$ ; $H_2O\% = 0.125$

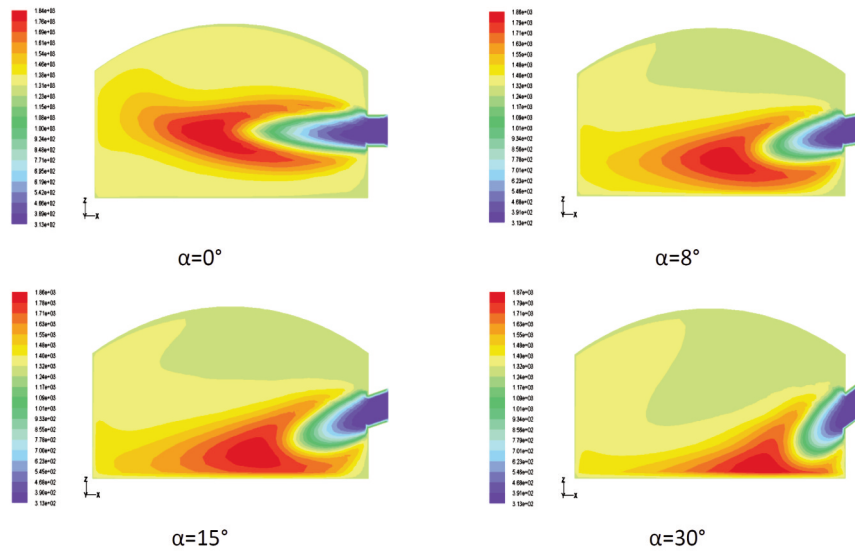


Figure 3. Sectional view of temperature fields of the center of Y axis with different  $\alpha$

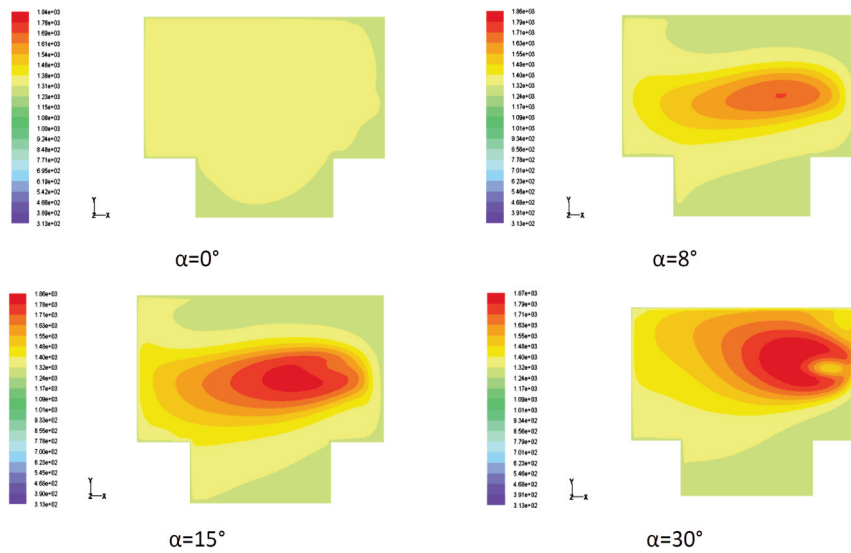


Figure 4. Sectional view of temperature fields of  $Z=25\text{mm}$  surface with different  $\alpha$

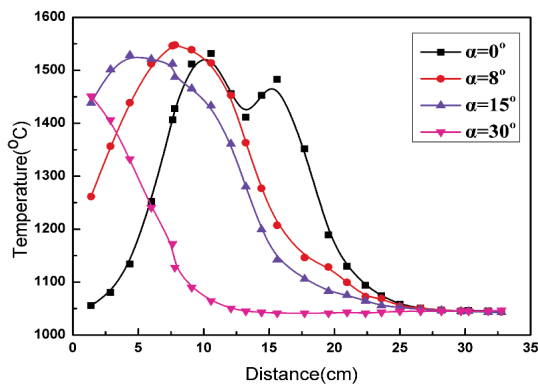


Figure 5. Temperature distribution on the center line

### 3. The reduction experimental with Multilayer pellets

#### 3.1 Raw material

Vanadium-titanium iron concentrate and coal were used as the raw material in this experiment. Their compositions were shown in Tables 3 and 4. The size distribution of the concentrate was shown in Table 5. Fig. 6 shows the XRD pattern of the vanadium-titanium iron concentrate from which we can see that the main phase in the ore were  $\text{Fe}_3\text{O}_4$ ,  $\text{Fe}_{2.75}\text{Ti}_{0.25}\text{O}_4$  and  $\text{FeTiO}_3$ .

**Table 3.** Chemical composition of iron concentrate/%

TFe	FeO	Fe <sub>2</sub> O <sub>3</sub>	SiO <sub>2</sub>	CaO	MgO	Al <sub>2</sub> O <sub>3</sub>	TiO <sub>2</sub>	S	P
53.95	31.61	41.95	3.31	1.14	2.62	3.96	12.81	0.75	0.0025

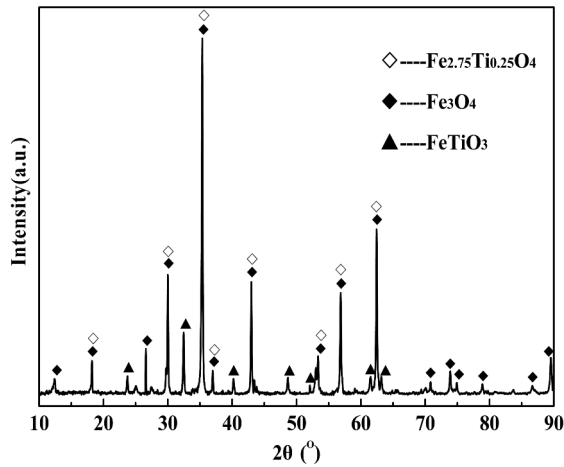
**Table 4.** Proximate and ultimate analysis of coal /%

Proximate analysis				Ultimate analysis
V <sub>ad</sub>	A <sub>ad</sub>	M <sub>ad</sub>	FC <sub>ad</sub>	St <sub>ad</sub>
12.02	18.41	7.33	62.24	0.44

Note: Proximate and ultimate analysis of sample under the air dry basis (ad).

**Table 5.** Size distribution of iron concentrate

mesh	32	32~60	60~100	100~150	150~200	200~320	-320
%	2.5	10	12.5	16.7	17.8	13	27.5

**Figure 6.** XRD pattern of iron concentrate

### 3.2 Experimental schedule

The vanadium-titanium iron concentrate and coal were mixed with  $C_{mol}/O_{mol}=1.2$ , the mixture was pressed into pellets with a diameter of 25mm and a height of 12.5mm under the pressure of 100MPa. The pellets were dried in the furnace for 6h with the temperature of 120°C. The amount of natural gas and air injected into the furnace was a fixed ratio. After the desired temperature of the furnace was reached, the pellets were loaded into the furnace quickly. The off-gas was first cooled and analyzed online by using the gas analyzer.

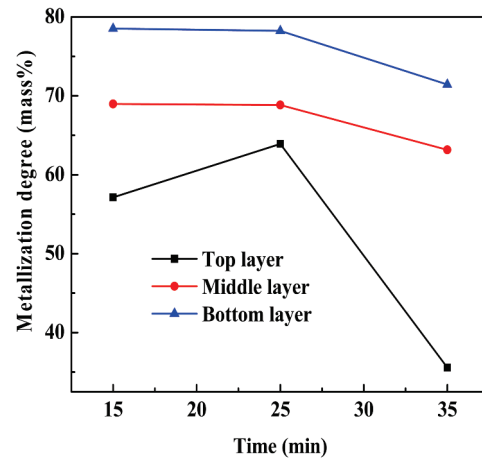
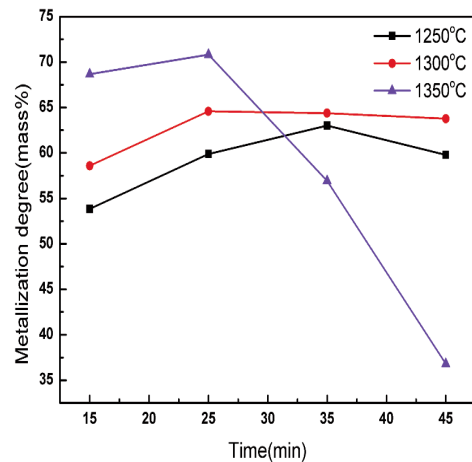
Three layers of pellets were used in the experiments. The reduction times were chosen as 15min, 25min and 35min respectively, and the reduction temperatures were chosen as 1250°C, 1300°C and 1350°C respectively.

## 4. Results and discussion

**Table 6.** Gas composition in the furnace

gas	CO	CO <sub>2</sub>	CH <sub>4</sub>	C <sub>n</sub> H <sub>m</sub>	H <sub>2</sub>	O <sub>2</sub>	N <sub>2</sub>
Volume fraction/%	0.02	11.46	0.12	0.18	0.12	0.64	87.46

Table 6 shows the atmosphere in the stable state furnace which indicates the strong oxidizing atmosphere in the furnace. Metallization of 3 layers pellets reduced at 1350 °C was shown in Fig. 7. For the pellets reduced for 25min, the metallization of the

**Figure 7.** Metallization of 3 layers pellets at 1350°C**Figure 8.** Average metallization of pellets at different temperatures

bottom layer was 9% higher compared with the middle layer and 14% higher compared with the top layer. When the time was prolonged to 35min, the metallization difference between the bottom and middle layer was merely changed while the difference between the bottom and top layer became larger.

Fig. 8 reveals the influences of reduction temperature and reduction time on the average metallization for 3 layers pellets [7]. The figure exhibited that with the increasing of the reduction time, the average metallization degree increased firstly and then decreased and get the maximum value at 25min, which is consistent with the reality operation. Analysis suggests that in the reduction process, the pellets reducing energy was mainly depended on the radiative transfer and was conveyed from the top to the bottom. In the initial stage, the top layer pellets were heated primary, the temperature of the bottom layer rise slowly due to the shelter from the top layer. During the reduction, the top layer pellets shrink in all directions. Thus, the top pellet-to-pellet distance increased and the radiating area of the middle layer pellets was enlarged. In the later stage, the middle and bottom layers pellets were reduced almost completely, however the top layer pellets were reoxidized by then. Thus there exists an optimal reduction time in order to get the maximum metallization in the process.

The pellet in the middle layer reduced at 1350°C for 15min was analyzed by scanning electron microscope,

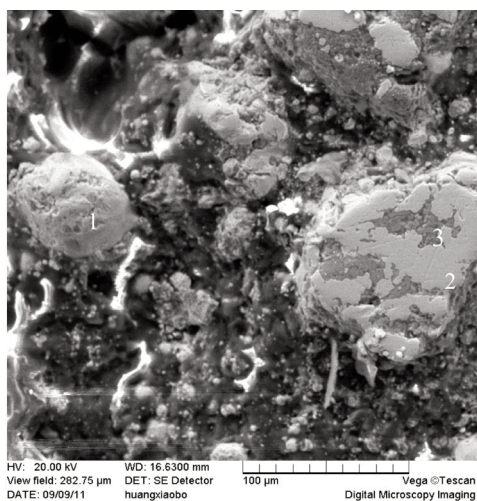


Figure 9. SEM of reduced pellet

Table 7. Point analysis of reduced pellet

Atomic percentage/%	Fe	Ti	C	O	V	Mg	Al	Ca	Si
1	55.28	0.23	39.14	4.61	0.19	0.04	0.14	0.13	0.25
2	82.26	0.35	11.92	3.36	0.19	0.08	0.34	0.03	1.45
3	0.66	24.39	2.99	62.6	0.19	2.27	2.48	1.22	3.19

which is shown in Fig.9 and Table 7. Table 7 illustrated that in point 2 Fe was present above 80 at%, which indicated to the aggregation area of Fe. The main elements in point 3 were Ti, O and small amount of other elements, which reveals it was the aggregation area of high TiO<sub>2</sub> slag [8]. The gathering Fe was also found in point 1, however the amount of C in point 1 was much higher than the other 2, which meant there was some residual carbon left in the pellet [9].

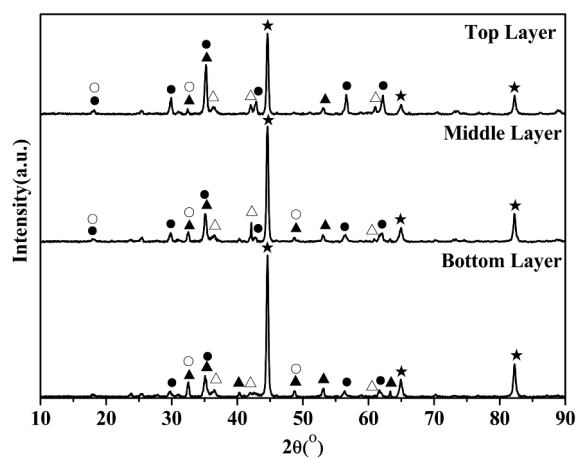


Figure 10. XRD patterns of pellets reduced at 1250°C for 25min

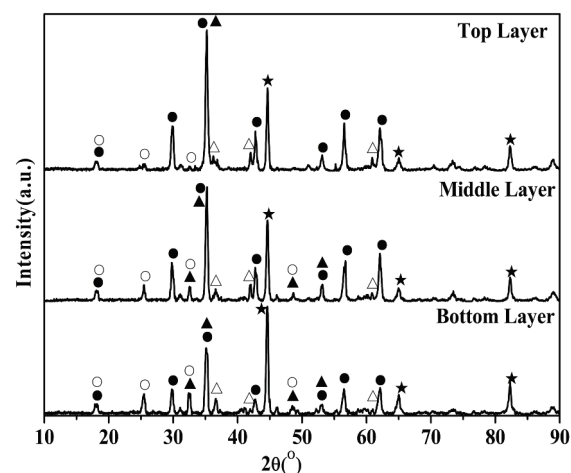


Figure 11. XRD patterns of pellets reduced at 1350°C for 25min  
 ★—Fe; ▲—FeTiO<sub>3</sub>;  
 △—FeO; ◯—FeTi<sub>2</sub>O<sub>5</sub>; ●—Fe<sub>2</sub>TiO<sub>4</sub>;  
 ◇—Fe<sub>2.75</sub>Ti<sub>0.25</sub>O<sub>4</sub>; ◆—Fe<sub>3</sub>O<sub>4</sub>; ▽—Fe<sub>2</sub>TiO<sub>5</sub>

It is reported [10] that two minerals in the pre-oxidized titanomagnetite were reduced gradually - the hematite took the road as follows:  $\text{Fe}_2\text{O}_3 \rightarrow \text{Fe}_3\text{O}_4 \rightarrow \text{FeO} \rightarrow \text{Fe}$ , while the pseudobrookite took the road according to:  $\text{Fe}_2\text{TiO}_5 \rightarrow \text{Fe}_2\text{TiO}_4 \rightarrow \text{FeTiO}_3 \rightarrow \text{FeTi}_2\text{O}_5 \rightarrow \text{Ti}_3\text{O}_5$ . The reduction process of the minerals in the iron concentrate lies in the above two processes [11]. The reduction difficulty [12] of iron-bearing minerals in vanadium-titanium iron concentrate increased by following order:



The XRD pattern of pellets reduced for 25min at 1250°C and 1350°C were shown in Fig. 10 and Fig. 11, respectively. The phases in the reduced pellet were mainly Fe and  $\text{Fe}_2\text{TiO}_4$  with a small amount of FeO,  $\text{FeTiO}_3$  and  $\text{FeTi}_2\text{O}_5$ . The relative intensity of Fe in the pellet reduced at 1250°C has a ascend tendency from the top layer to the bottom layer which reveals the top layer pellets were reoxidized to some extent. With the temperature rise, the relative intensity of Fe in the pellet reduced at 1350°C which was weaker compared with the case of 1250°C, while the relative intensity of  $\text{FeTiO}_3$  and  $\text{Fe}_2\text{TiO}_4$  become stronger. The phenomenon can be attributed to the higher temperature which promoted the reaction, then the reduced Fe was reoxidized and titanium oxide begun to be reduced.

## 5. Conclusions

Following conclusions can be given:

1. With  $\alpha$  increases, the high temperature field become larger on the surface of  $Z=25\text{mm}$  in the prehearing area of RHF. However, the high temperature field on the vertical direction will move down and present a shrinking tendency. The proper inlet angle of the nozzle in this study was 15° in which case the burden in the furnace can be heated to the reduction temperature in a relatively shorter time.

2. For the pellets reduced at 1350°C for 25min, the metallization of the bottom layer was 9% higher compared with the middle layer and 14% higher compared with the top layer.

3. The average metallization of multilayer pellets is in positive proportion to the experimental temperature. With the reduction time increase, the average metallization degree increased firstly and then decreased. The top layer pellets would be reoxidized while the middle and bottom layer pellets were being reduced. With the number of layers increased, the nonsimultaneous situation become more obviously. The average metallization of the pellets in the experiment get the maximum value at 25 min which is consistent with the reality operation.

For the future study, another constructive thinking raised to further improve the energy utilization efficiency of RHF. In consideration of the

nonsimultaneous reduction in the furnace, the different size pellets and catalytic agent will be used. For the top layer pellets, larger pellets will be employed due to the quick reduction property; smaller and catalytic agent addition pellets correspondingly will be employed for the bottom layer.

## Acknowledgment

*The authors are especially grateful to the Key Project of Chinese National Programs for Fundamental Research and Development plan (No. 2013CB632603).*

## References

- [1] Z.F. Yuan, Y.F. Pan, E. Zhou, C. Xu, S.Q. Li. J. Iron. Steel Res. Int., 14 (1) (2007) 1-6.
- [2] L.H. Zhou, D.P. Tao, M.X. Fang, F.H. Zeng, X. Pu. Chin. J. Rare. Met., 3 (2009) 406-410.
- [3] J. Qin, X. Xue, J. Deng. Res. Iron. Steel, 337 (2011) 125-132.
- [4] H. Lu, J. Xu, Q. Li. Proc. of 2012 TMS Annual Meeting. 15-19 March, Florida, USA, 2012, p.109-116.
- [5] W.K. Lu, D. Huang. Miner Process Extr. M., 24 (3) (2003) 293-324.
- [6] Z.H. Zhong, W.M. Zhao, X.D. Xie. Adv. Mater. Res., 15 (2014) 1297-1300.
- [7] K. Nagata, R. Kojima, T. Murakami, M. Susa, H. Fukuyama. ISIJ Int., 41 (11) (2001) 1316-1323.
- [8] M. A. R. Dewan, G. Zhang, O. Ostrovski. Metall. Mater. Trans. B, 41 (1) (2010) 182-192.
- [9] E. Kasai, T. Kitajima, T. Kawaguchi. ISIJ Int., 40 (9) (2000) 842-849.
- [10] S. Ranganathan, K. Bhattacharyya, A. Ray, K. Godiwalla. Miner. Process. Extr. M., 121 (1) (2012) 55-63.
- [11] X.F. She, H.Y. Sun, X.J. Dong, Q.G. Xue, J.S. Wang, J. Min. Metall. Sect. B-Metall. 49 (3) B (2013) 263-270.
- [12] S. K. Gupta, V. Rajakumar, P. Grieveson. Metall. Mater. Trans. B, 22 (5) (1991) 711-716.